Determination of Resistance Coefficient and Turbulent Friction Factor in Non-Circular Ducts*

Habib UMUR**

Static pressures in non-circular ducts and pipe fittings (globe, ball and butterfly valves) have been measured in a closed circuit water channel at the range of Reynolds number from 20 000 to 80 000, which give rise to fully developed turbulent pipe flow, so as to define the friction coefficient (C_f) and resistance coefficients (K). A new proposed equation for friction factor with two new dimensionless parameters as a function of cross sectional area are successfully adopted to fully developed turbulent flow in all cross sections with a precision of better than $\pm 4\%$. Measurements showed that friction factors decreased with increasing eccentricity and were in good agreement with the proposed equation. It was also found out that Reynolds number has no effect on resistance coefficients of butterfly, globe and gate valves, but the closing ratio caused K to increase remarkably, and the K value of bends can easily be obtained by an empirical formula based on Moody chart friction factor. Static pressures on front and back sides of the circular disc of butterfly valve decreased with Reynolds number, remained almost constant in the radial direction and increased particularly at closing angles of bigger than 60 degrees, where flow rate starts to decrease sharply.

Key Words: Friction Factor, Resistance Coefficients, Valves, Turbulent Flows, Non-Circular Ducts

1. Introduction

Definition of friction coefficient in fully developed flows has been the subject of many studies, most of which have been experimental and empirical. There is no acceptable and applicable correlation particularly on non circular duct flows since the hydraulic diameter is insufficient to describe the skin friction. Beside the hydraulic diameter, the friction factor is dependent on Reynolds number, duct geometry and boundary conditions, which are very difficult to produce particularly in rectangular, elliptical, triangular, concentric and eccentric annular ducts etc.

Exact solutions of the laminar continuity and momentum equations are obtained for some simple geometries, such as the circular tubes, parallel plates, concentric and eccentric annular ducts. Since there is no such a solution in turbulent flows, approximation methods such as universal velocity profile and effective diameter is suggested for a better understanding of the flow phenomenon. The wall friction in rectangular and triangular laminar duct flows decreases from the midpoints of the side, where the friction is maximum, to the corners where there is no friction. For turbulent flows, the wall friction remains nearly constant along the sides but becomes suddenly zero in the corners, due to secondary flow cells in the plane of the cross-section.

The pressure losses in pipe fittings (pipe entrance and exit, expansions and contractions, elbows and valves etc.) and curved pipes can be much greater than a long pipe due to the complexity of the flow. Since there is no theory in these types of flows, skin friction is obtained either experimentally or empirically.

The knowledge of the flow in non-circular pipes has been investigated by Brundett and Bains[1], Gessner and Jones[2], Melling and Whitelaw[3] in rectangular ducts and by Brighton and Jones[4], Jonsson and Sparrow[5], Qurmby[6], Kacker[7], Lawn and Elliott[8], Rehme[9], Jones and Leung[10], Umur[11] and Nouri et al.[12] in concentric and eccentric annuli and the resistance coefficients by Igarashi and Inagaki[13] and

* Received 6th May, 1999
** Mechanical Engineering Department, Engineering and Architecture Faculty, Uludag University, 16059 Bursa, Turkey. E-mail: umur@uludag.edu.tr

Igarashi[14]. The present study describes skin friction in non-circular ducts and flow resistance in butterfly, globe and ball valves and presents a simple and reliable new equation for the calculation of turbulent friction coefficient in all types of cross sectional shapes.

Nomenclature

A : projected area of the circular disc, m^2
A_0 : cross sectional area, m^2
C_f : skin friction factor, dimensionless
d : pipe diameter, mm
d_{eff} : effective diameter, mm
d_h : hydraulic diameter, mm
d_m : maximum diameter, mm
d_1 : inner pipe diameter, mm
d_2 : outer pipe diameter, mm
e : eccentricity, mm
K : flow resistance, dimensionless
P_1 : upstream static pressure, N/m^2
P_2 : downstream static pressure, N/m^2
Re : Reynolds number, dimensionless
Re_h : hydraulic Reynolds number, dimensionless
Re_{eff} : effective Reynolds number, dimensionless
R : radius of curvature, mm
r_1 : inner radius, mm
r_2 : outer radius, mm
r^* : radius ratio, dimensionless
U : mean velocity, m/s

Greek

α : a ratio of real area to maximum area based on d_m, dimensionless
α_1 : closing ratio (A/A_0), dimensionless
β : a ratio of d_h to d_m, dimensionless
φ : duct geometry coefficient, dimensionless
ν : kinematic viscosity, m^2/s
θ : closing angle, degrees

2. Experimental Apparatus and Flow Conditions

A horizontal rig was constructed with butterfly, globe and ball valves as shown in Fig. 1 and carefully changed to be eccentric or square duct as required. The closed circuit water channel comprised globe, ball and butterfly valves, a constant speed pump which delivered the water from a supply tank with a by-pass loop to control the flow rate (Fig. 2). The outer diameter of the eccentric annuli of 2.5 m length was 100 mm with a diameter ratio $(r^*=r_1/r_2)$ of 0.5 and eccentricities $(e=1/(r_2-r_1))$ of 0.00, 0.5 and 1.0. Where l is the distance between the center of the outer and inner pipes, r_2 and r_1 refer to outer and inner pipe radius. The square duct has also 2.5 m length and 40×40 mm^2 cross sectional area. All pipes were made of copper and the temperature of water was controlled to 25°C to eliminate the viscosity effects. The bulk flow velocity was measured with a calibrated orifice plate with a precision of 2%. Static pressure distribution on the front and back sides of the clap (see Fig. 3) were also measured in radial and tangential directions.

Static pressure measurements were obtained from pressure taps located both longitudinally and

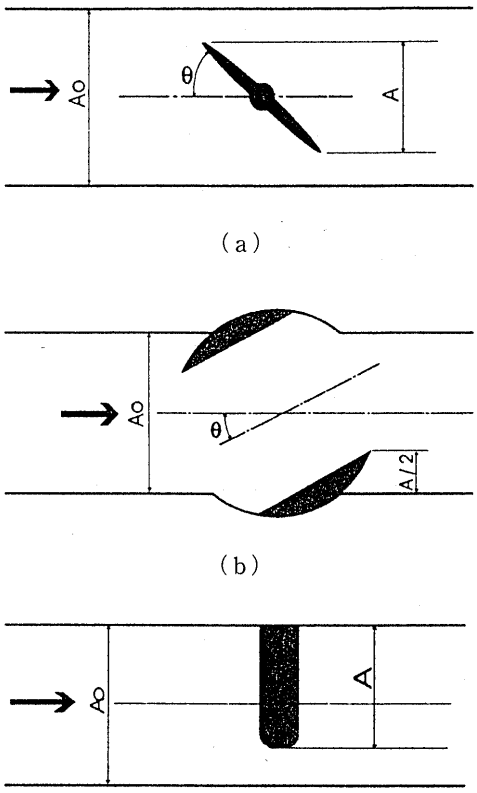

Fig. 1 Cross sectional area of valves, (a) butterfly valve, (b) globe valve, (c) gate valve

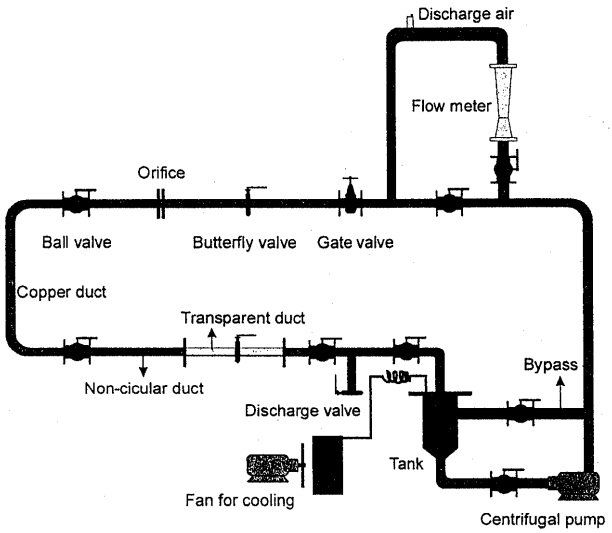

Fig. 2 Experimental set up

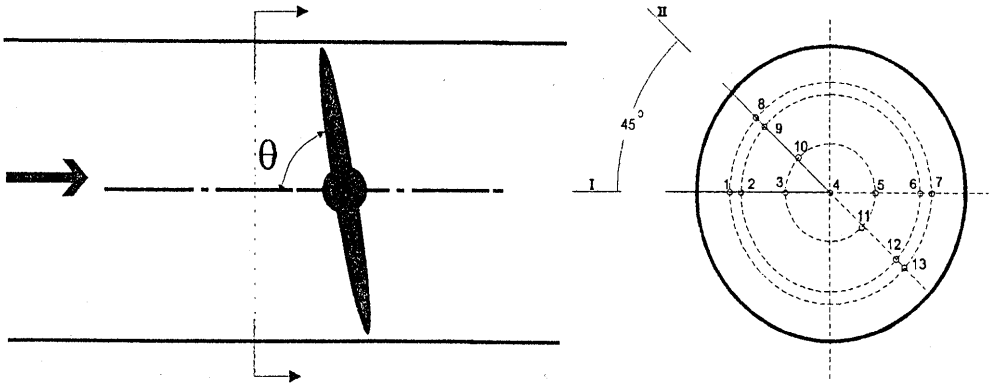

Fig. 3 Static pressure locations on the butterfly disc

circumferencially. They were read from a calibrated manometer bank with ∓1 mm resolution. The specific density of the manometer fluid was 1 800 kg/m^3 giving a height range of 20 to 1 000 mm. The Reynolds number based on the hydraulic diameter range of the investigation extended from 20 000 to 80 000 to ensure fully developed turbulent flow and to provide data with the correlation methods.

3. Proposed Correlation Methods

The inefficiency of the hydraulic diameter both for laminar and turbulent flows requires additional geometric parameters for the accurate prediction of frictional pressure drops. The laminar based length dimension to correlate the turbulent friction factors have been used by Rehme[9] Fredrickson and Bird[15], and Meter and Bird[16], by Quarmby[17], Jones[18] and others in non-circular ducts. The fully developed friction factor can be obtained from the equation of definition

$$C_f=\frac{dP}{dx}\frac{d_h}{2\rho U^2} \tag{1}$$

in which dP/dx and U show static pressure difference and bulk velocity, respectively. For instance, the friction factor for laminar pipe flow is defined as

$$C_f=16/Re_h \tag{2}$$

and C_f for turbulent pipe flow is for $10\,000<Re_h<50\,000$,

$$C_f=0.079Re_h^{-0.25} \tag{3}$$

and for concentric annuli by Rothfus[19], $C_f=0.087Re_h^{-0.25}$. The friction factor obtained by evaluating Eq.(1) has been simply correlated by a power-law relationship of the type

$$C_f=CRe_h^{-n} \tag{4}$$

where $Re_h\left(Re_h=\frac{Ud_h}{\nu}\right)$ is the Reynolds number based on the hydraulic diameter (d_h), C is a constant and n is the power law index.

The line of best fit proposed by Nouri et al.[12] is $0.36Re_h^{-0.39}$ for concentric annuli and $0.28Re_h^{-0.39}$ for unit eccentricity which were some 11% higher and 14% lower than the pipe flow, respectively. These results clearly shows that each cross section has to be presented by a different equation so that a new correlation which is valid for all kinds of cross section is of vital importance for simplicity and reliability. Here, an effective Reynolds number based on effective diameter ($d_{\text{eff}}=d_h/\varphi$) rather than hydraulic Reynolds number will be used for calculations as

$$Re_{\text{eff}}=\frac{Ud_{\text{eff}}}{\nu}=\frac{Re_h}{\varphi} \tag{5}$$

where φ is a duct geometry coefficient for fully developed flows. φ needs to be calculated for each non-circular duct flow case such as rectangular, triangular, elliptical and eccentric ducts, which is very complicated even in a particular duct flow so that a new equation has to be defined in order to describe φ for all types of cross sectional shapes for fully developed flows. For this reason, φ values in the literature of Shah and London[20] and present experimental results have been presented as functions of new parameters of β and α (see Fig. 4) and then new equation is proposed by, for $\beta<1$

$$\varphi=\left(\frac{\beta}{\alpha}\right)^{0.5} \tag{6}$$

and for $\beta>1$

$$\varphi=1+\left(\frac{\alpha-1}{\alpha}\right)^{2/3}\left(\frac{\beta}{3}-\frac{2}{3\beta^2}\right) \tag{7}$$

where β and α are the new dimensionless parameters to describe the flow area as,

$$\beta=\frac{d_h}{d_m} \quad \text{and} \quad \alpha=\frac{A}{\pi d_h^2/4} \tag{8}$$

in which d_m refers to diameter of the maximum circular duct inside the cross sectional area of A. As can be seen from Fig. 4, the only difference resulted from the calculation of φ for triangular duct geometry for $\beta=1$ (dashed line in Fig. 4) which has bigger duct geometry coefficient so that two different values for $\beta=1$ is the main reason of maximum ±4% error in extreme cases.

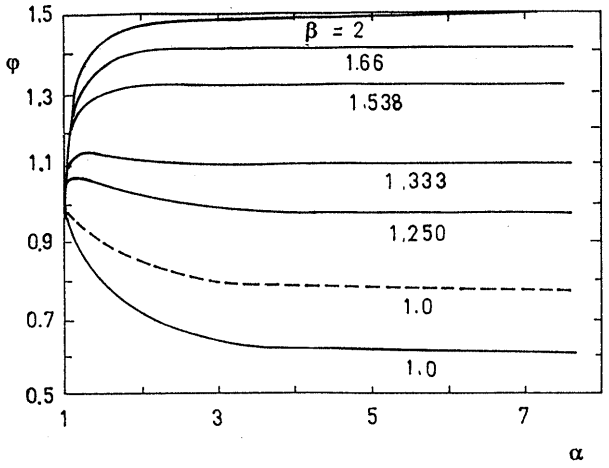

Fig. 4 Duct geometry coefficient as functions of α and β

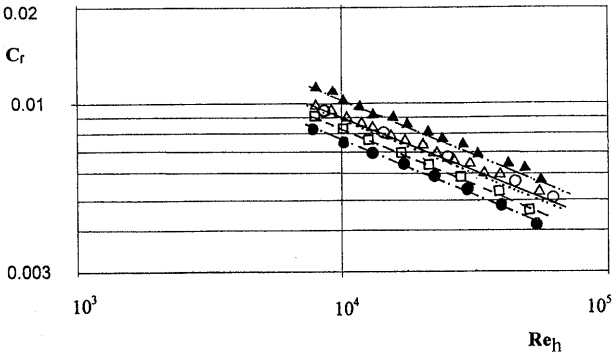

Fig. 5 Friction factor with hydraulic Reynolds number ·····○: Circular duct, ------□: Square duct, ——▲: Concentric, ————△: Eccentricity of 0.5, ——●: Unit eccentricity

4. Results and Discussion

Static pressure measurements are presented for concentric, eccentric and square duct flows and on the front and back sides of the butterfly clap together with resistance coefficients for butterfly, globe and ball valves and curved pipes separately.

The results of pipe flow skin friction factor lie close to the relation for the plain tube, i.e. $C_f=0.32\,Re_h^{-0.39}$ and the concentric values are close to $C_f=0.32\,(Re_h/\varphi)^{-0.39}=0.36Re_h^{-0.39}$ respectively, as shown in Fig. 5. The results obtained from Eq.(7) for concentric annuli is also in good agreement with equations of Brighton and Jones[4] with ±1%, and Nouri et al.[12], within 3% and some 13% higher than those of smooth pipe results. Where $\varphi=1.381$ from Eq.(7) for $r^*=0.5$, $\alpha=3$, $\beta=2$ concentric annuli. The results for duct flow ($\varphi=0.89$ from Eq.(7) for $\alpha=1.273$, $\beta=1$) gave $C_f=0.32(Re_h/\varphi)^{-0.39}=0.306\,Re_h^{-0.39}$ which is 5% less than pipe flow ($\varphi=1$), measurements. The results for the higher Reynolds numbers ($3\times10^4<Re<10^6$) can be presented by $C_f=0.046(Re_h/\varphi)^{-0.20}$.

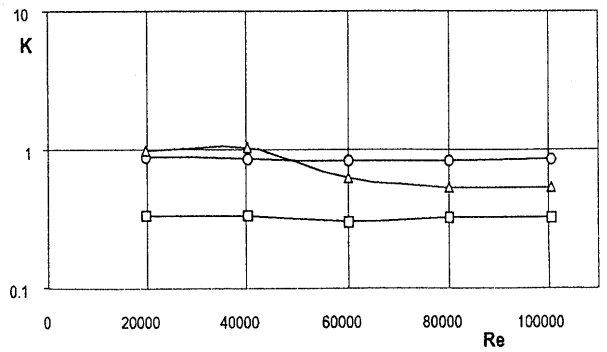

Fig. 6 Resistance coefficients versus Reynolds number ○: Globe, □: Gate, △: Butterfly valves

Measurements with eccentricities of 0.5 and 1.0 are shown in Fig. 5. Experimental skin friction factors are in accord with equation of $C_f=0.33(Re_h)^{-0.39}=0.32(Re_h/\varphi)^{-0.39}$ for $\varphi=1.053$ from Eq.(7) $e=0.5$, $\alpha=3$ and $\beta=1.333$. The results are also in good agreement with equation of $C_f=0.89(Re_h)^{-0.39}=0.32(Re_h/\varphi)^{-0.39}$ for $\varphi=0.74$ from Eq.(7) for $e=1.0$, $\alpha=3$ and $\beta=1.0$, and are 3% higher for $e=0.5$ and 12.5% lower for $e=1.0$ than smooth pipe flow values. The skin friction factors based on the proposed equation of (7) are in good agreement with those of experimental results with a precision of less than ±2%. The measured values and Eq.(7) clearly show that the lines of best fit proposed by Nouri et al.[12] for skin friction factors in concentric and eccentric annuli can exactly be obtained through φ values of 1.381 for concentric ($C_f=0.32(Re_h/\varphi)^{-0.39}=0.36\,Re_h^{-0.39}$), of 1.053 for $e=0.5$ ($C_f=0.33Re_h^{-0.39}$) and of 0.74 for unit eccentricity ($C_f=0.28Re_h^{-0.39}$).

The results showed that duct geometry coefficient can successfully be obtained through Eq.(7) within ±4% and the skin friction coefficient in turbulent flows together with the definition of φ of Eq.(7) can easily be computed as

$$C_f=0.32(Re_h/\varphi)^{-0.39} \qquad (9)$$

The skin friction decreases with increasing eccentricity and reaches the lowest value at unit eccentricity, which is in accord with the results of Jonsson and Sparrow[5], Kacker[7], Umur[11] and Nouri et al.[12]

The flow resistance coefficient K was obtained by

$$K=\frac{P_1-P_2}{0.5\rho U^2} \qquad (10)$$

where P_1 and P_2 refer to static pressures measured $2d$ upstream and $6d$ downstream from the center of the valve. The effect of Reynolds number ($Re=Ud/\nu$) on resistance coefficients of butterfly, globe and ball valves for fully open conditions are presented in Fig. 6. Where d refers to pipe diameter. There is no remarkable effect of the Reynolds number on K, but the value of K for gate valves are slightly smaller

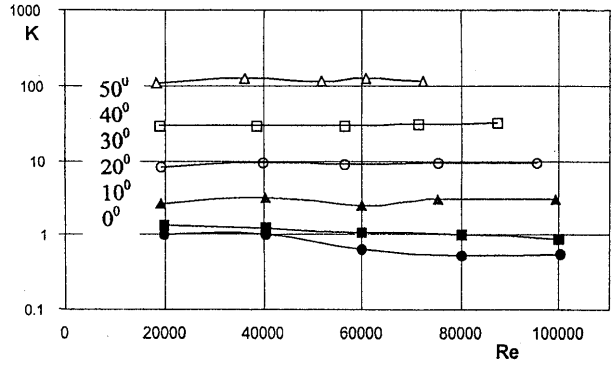

Fig. 7 The influence of closing ratio in K values

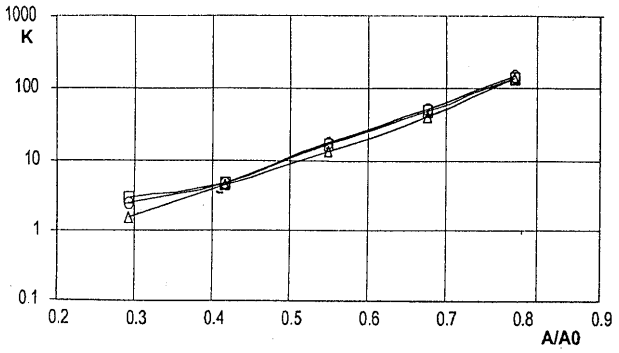

Fig. 8 Effect of closing ratio and Reynolds number on resistance coefficients (for symbols, see Fig. 6)

than those of butterfly and globe valves with increasing Reynolds numbers.

The effect of Reynolds number and the closing ratio a_1 on the resistance coefficients of butterfly valve is shown in Fig. 7. Where a_1 is the ratio of projected area $\left(A=\frac{\pi d^2}{4}\sin\theta\right)$ to fully open area $\left(A_0=\frac{\pi d^2}{4}\right)$ and θ is the closing angle. The coefficient of resistance increases with closing ratio but remains almost constant with Reynolds number which is in good agreement with the results of Igarashi and Inagaki[13]. For instance, K is almost 10 times smaller at the half close position of $a_1=0.5$ ($\sin\theta=30°$) than those of 80% close position. The results showed that the closing ratio gave rise to larger K values for all three valves as seen in Fig. 8. The butterfly valve has less resistance coefficients than globe and ball valves in partially open conditions.

A bend or curve in a pipe induces larger losses than the simple friction loss due to flow separation at the walls and a swirling secondary flows arising from the centrifugal forces. The influence of curvature is shown in Fig. 9. The bend resistance K decreased with R/d and increased with ε/d. By analyzing all data and Moody chart, the simple new equation as a function of C_f (straight pipe flow friction factor from Moody chart) has been proposed to calculate K as,

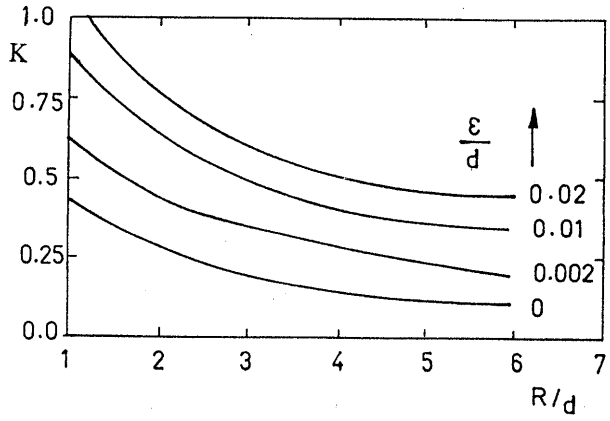

Fig. 9 Resistance coefficients for bends

$$K=\frac{\Delta P}{0.5\rho U^2}=90C_f\sqrt{\frac{d}{R}} \tag{11}$$

where d is the pipe diameter, R is the radius of curvature, ε is the surface roughness and ε/d is the relative roughness. Equation (11) is in good accord with the measured values with an error of $\pm 2\%$.

Static pressures are shown in Figs. 10(a) and (b) on the front sides of the circular disc and in Figs. 10(c) and (d) on the back sides in directions of I and II (Fig. 3), respectively. Static pressures on the front side are larger than those at back side and no considerable change on the static pressure in the radial direction has been recorded up to closing angle of 60°, but increased around 50% at closing angle of 80°. This is partly because of the sharp decrease in the flow rate after the closing angle of 60 degrees. Static pressures on both sides decreased with increasing Reynolds number. The radial variation of static pressure at plane 1 and plane II is almost constant up to 60° closing angle on both sides, but increased remarkably on upper section of the back side at closing angle of 80°, due to strong separation of the flow of upper part.

5. Conclusions

The results showed that the skin friction for any type of duct geometry can easily be presented as functions of α and β so that the friction factor in non-circular ducts can successfully be calculated for fully developed flows. Experimental skin friction coefficients are in good agreement with the proposed equation with a maximum error of $\pm 4\%$. The variation of skin friction coefficient with Reynolds number shows that the flow resistance increases with concentric annuli by 13% compared to smooth pipe flow and decreases with increasing eccentricity, and hence skin friction factor with an unit eccentricity is 12.5% less than pipe flow and 22% less than concentric annuli. Resistance coefficients of all valves remained almost

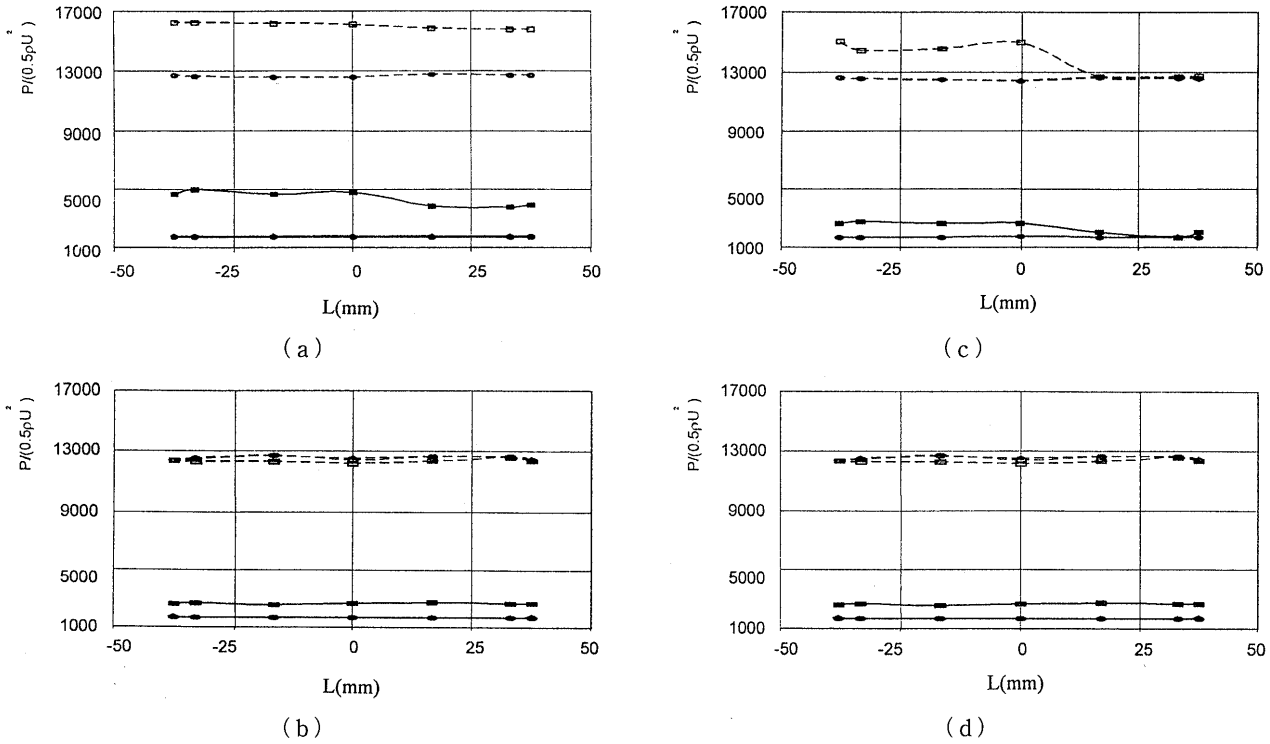

Fig. 10 Static pressure distribution on the butterfly discs (a) front side in the radial direction of I, (b) front side in the radial direction of II, (c) back side in the radial direction of I, (d) back side in the radial direction of II
—●: 40°, —◆: 60°, —■: 80° for Re=40 000
·····○: 40°, ·····◇: 60°, ·····□: 80° for Re=20 000

constant with increasing Reynolds number, but increases remarkably with closing ratio. The results also showes that the K value of bends can successfully be calculated through straight pipe flow friction factors. The static pressure on the circular disc increases with closing angle particularly after 60° of closing and decreased with increasing Reynolds number for the butterfly valve.

Acknowledgments

The author is glad to express his thanks to the ELMAK Ltd. in Bursa for financial support and to Research Eng. Mustafa Bariş for his assistance during the conduct of experiments.

References

(1) Brundett, E. and Bains, W.D., The Production and Diffusion of Vorticity in Duct Flow, Journal of Fluid Mechanics, Vol. 19 (1964), p. 375.
(2) Gessner, F.B. and Jones, J.B., On Some Aspects of Fully Developed Flow in Rectangular Channels, Journal of Fluid Mechanics, Vol. 24 (1965), p. 689.
(3) Melling, A. and Whitelaw, J.H., Turbulent Flow in Rectangular Duct, Journal of Fluid Mechanics, Vol. 78 (1976), p. 289.
(4) Brighton, J.A. and Jones, J.B., Fully Developed Turbulent Flow in Annuli, ASME Journal of Basic Engineering, Vol. 86 (1964), p. 19.
(5) Jonsson, V.K. and Sparrow, E.M., Experiments on Turbulent Flow Phenomena in Eccentric Annular Ducts, Journal of Fluid Mechanics, Vol. 25 (1966), p. 65.
(6) Qurmby, A., An Experimental Study of Turbulent Flow Through Concentric Annuli, Ins. J. Mech. Sci., Vol. 9 (1967), p. 205.
(7) Kacker, S.C., Some Aspects of Fully Developed Turbulent Flow in Non Circular Ducts, Journal of Fluid Mechanics, Vol. 57 (1973), p. 583.
(8) Lawn, C.L. and Elliott, C.J., Fully Developed Turbulent Flow Through Concentric Annuli, J. Mech. Eng. Sci., Vol. 14 (1972), p. 195.
(9) Rehme, K., Simple Method of Predicting Friction Factors of Turbulent Flow in Non-Circular Channels, Int. J. Heat Mass Trans., Vol. 16 (1973), p. 933.
(10) Jones, O.C. and Leung, J.C.M., An Improvement in the Calculation of Turbulent Friction in Smooth Concentric Annuli, ASME Journal of Fluids Engineering, Vol. 103 (1981), p. 615.
(11) Umur, H., Flows with Curvature, PhD Thesis, London University, Imperial College, London, (1991).
(12) Nouri, J.M., Umur, H. and Whitelaw, J.H., Flow of Newtonian and Non-Newtonian Fluids in Concentric and Eccentric Annuli, Journal of Fluid

Mechanics, Vol. 253 (1993), p. 617.
(13) Igarashi, T. and Inagaki, S., Hydraulic Losses of Flow Control Devices in Pipes, JSME Int. J., Ser. B, Vol. 38, No. 3 (1995), p. 298.
(14) Igarashi, T., Flow Resistance of a Vortex Shedder in a Circular Pipe, 5. Triennial International Symposium on Fluid Control, Measurement and Visualization, Sept. 1-4, Hayama, Japan, (1997).
(15) Fredrickson, A.G. and Bird R.B., Friction Factors for Axial Non-Newtonian Annular Flow, Ind. and Eng. Chem. Vol. 50 (1958), p. 1599.
(16) Meter, D.M. and Bird, R.B., Turbulent Newtonian Flow in Annuli, AICHE Journal, Vol. 7 (1961), p. 41.
(17) Quarmby, A., An Analysis of Turbulent Flow in Concentric Annuli, Appl. Sci. Re., Vol. 19 (1968), p. 250.
(18) Jones, O.C., An Improvement in the Calculation of Turbulent Friction in Rectangular Ducts, ASME Journal of Fluids Engineering, Vol. 98 (1976), p. 173.
(19) Rothfus, R.R., Velocity Distribution and Fluid Friction in Concentric Annuli, Sc. D. Thesis, Carnigie Inst. Tech. (1948).
(20) Shah, R.K. and London, A.L., Laminar Flow Forced Convection in Ducts, (1978), Academic Press, New York.